Wind and Structures, *Vol. 22, No. 4 (2016) 503–524*
DOI: http://dx.doi.org/10.12989/was.2016.22.4.503

Wind flow simulations in idealized and real built environments with models of various level of complexity

Daniel S. Abdi* and Girma T. Bitsuamlak[a]

Department of Civil and Environment Engineering, University of Western Ontario, London, ON, Canada

(Received June 10, 2015, Revised February 9, 2016, Accepted February 13, 2016)

Abstract. The suitability of Computational Fluid Dynamics (CFD) simulations on the built environment for the purpose of estimating average roughness characteristics and for studying wind flow patterns within the environment is assessed. Urban models of various levels of complexity are considered including an empty domain, array of obstacles arranged in regular and staggered manners, in-homogeneous roughness with multiple patches, a semi-idealized built environment, and finally a real built environment. For each of the test cases, we conducted CFD simulations using RANS turbulence closure and validated the results against appropriate methods: existing empirical formulas for the homogeneous roughness case, empirical wind speed models for the in-homogeneous roughness case, and wind tunnel tests for the semi-idealized built environment case. In general, results obtained from the CFD simulations show good agreement with the corresponding validation methods, thereby, giving further evidence to the suitability of CFD simulations for built environment studies consisting of wide-ranging roughness. This work also provides a comprehensive overview of roughness modeling in CFD-from the simplest approach of modeling roughness implicitly through wall functions to the most elaborate approach of modeling roughness explicitly for the sake of accurate wind flow simulations within the built environment.

Keywords: CFD; built environment; wind flow; roughness; urban models

1. Introduction

Atmospheric Boundary Layer (ABL) flow is affected by aerodynamic roughness that comprises of both the effects of surface cover (roughness) and that of the terrain (topography). Form drag due to topographic features, such as hills and escarpments, contribute the most to modification of ABL flow (Abdi and Bitsuamlak 2014b). The urban built environment, that is considered part of surface cover, can also have a significant effect on wind flow characteristics especially in city centers where buildings are tall and densely populated (Hansen 1993). The Davenport *et al.* (2000) roughness classification, which is based on land-use, is commonly recommended in building codes and standards for the purpose of estimating average surface roughness characteristics of a given site. In cases where detailed wind mapping of the area is sought, experimental methods, such as field measurements and

*Corresponding author, Ph.D., E-mail: dshawul@yahoo.com
[a]Associate Professor, E-mail: gbitsuam@uwo.ca

http://www.techno-press.org/?journal=was&subpage=8 ISSN: 1226-6116(Print), 1598-6225(Online)

Boundary Layer Wind Tunnel (BLWT) testing on a scaled model, are often employed. However, numerical studies can prove to be cheaper alternatives to experimental studies. CFD has been successfully used for environmental studies such as pollutant dispersion and pedestrian wind comfort (Blocken and Carmeliet 2004a, Huang *et al.* 2008, Tominaga and Stathopoulos 2011). Discussion of other environmental applications of CFD can be found in Wright and Hargreaves (2013). Modeling the wide variety of roughness in the built environment is a challenging task, because most of the existing empirical methods are limited to moderately rough terrain. Recently, Aboshosha *et al.* (2015) used an approach of modeling rough terrain using fractal surfaces generated from random Fourier modes. To verify the viability of their approach, they conducted LES simulations using the resulting equivalent roughness models. In this work, we use both implicit and explicit roughness modeling approaches depending on the level of roughness. Even though explicit roughness modeling can be computationally intense, and probably not recommendable for slightly rough terrain, it can yield more accurate predictions of wind profiles within the built environment.

Blocken and Carmeliet (2004a) group numerical studies on the built environment into two categories: (a) fundamental studies on simple and generic building configurations (b) applied studies on complex case studies. Fundamental studies on isolated cases help to understand flow behavior in and around a building, and also to validate CFD codes against wind tunnel and field measurements. Blocken *et al.* (2011b) have reviewed the current status of CFD in building performance studies of outdoor environment. Currently, the four main application areas of CFD are pedestrian wind comfort and wind safety, pollutant dispersion, wind driven rain and convective heat and mass transfer studies. The first two applications of CFD have enjoyed wide spread use; however, its application to the other two areas is still not very popular. A case study of CFD simulation for pedestrian comfort in a University campus is described in Blocken *et al.* (2011a). The paper describes a general simulation and decision framework for the evaluation of pedestrian wind comfort and wind safety in urban areas using CFD. Numerical studies concerning particle transport by the mean flow field, such as dispersion and deposition of pollutants and moisture-related damage of buildings due to wind-driven rain, have also been done in the past by several researchers. Pollutant dispersion studies using CFD can be found in Huang *et al.* (2008), Tominaga and Stathopoulos (2011), and wind-driven rain studies using CFD can be found in Blocken and Carmeliet (2002), Tang and Davidson (2004) among many others. Wind-driven rain studies using CFD are especially time consuming because of the need of Lagrangian particle tracking of rain-drops, and also due to the fact that accurate simulation of turbulent dispersion of rain-drops requires Large Eddy Simulation (LES) instead of Reynolds Averaged Navier-Stokes (RANS). Thus, experimental and empirical investigation of such complex phenomenon have been the automatic choice for several years (see e.g., Asghari (2014) for experimental studies). Experimental investigation of pollutant dispersion has been done much earlier than CFD investigation of the phenomenon by Hall *et al.* (1996), Theurer (1993) among others. A review of experimental and semi-empirical studies of wind-driven rain can be found in Blocken and Carmeliet (2004b).

Due to the complexity of the phenomenon, built environment studies are usually focused on two simplified models : urban street canyon and isolated building. Although there are some studies on complex urban environments, the general lack of extensive validation is a serious problem towards standardization of CFD. However, the general consensus is that CFD can be used to avoid at least the preliminary stages of investigation, in which many parametric studies can be conducted with relative ease compared to experimental methods.

This study attempts to gauge performance of CFD for predicting wind flow in outdoor environments of various complexity without focusing on a particular application, i.e., disregarding tracers such as pollutants or rain that may be carried by the flow. The background flow field is the driver mechanism for tracer transport; thus, adequate prediction of the urban flow field is crucial. The metric we use for comparing CFD against empirical models and experimental data are average roughness parameters calculated from the flow field, namely roughness length and displacement height, and wind speed measurements at specific locations that maybe of particular concern for pedestrian wind comfort studies.

The remainder of the paper is organized as follows. In section 2, the built environment test cases of different complexity are described starting from the simplest case with no obstacles. The choices made for conducting the CFD simulations: type of turbulence model, grid generation, domain size are also described in the same section. In sections 3 through 7, we consider the five test cases one by one. A detailed description of the test setup, boundary conditions, and results are given for each case. Finally general observations and conclusions about performance of CFD for the outdoor built environment simulations are given in section 8.

2. Description of test cases and CFD simulation setup

This work examines wind flow characteristics in the built environment by conducting CFD simulations over idealized and real built environment configurations of different levels of complexity. The categorization of case studies based on complexity, shown in Fig. 1, follows closely the one used in CEDVAL-LES (2011) database, a compilation of wind-tunnel tests for validation of LES based numerical flow and dispersion models. However, only the case of the semi-idealized built environment uses the same model as that found in the CEDVAL database. In the following, we describe briefly the different categories and corresponding validation methods. A detailed description of the test setup for each case is given in sections 3 through 7.

Complexity 0, Empty domain: This is a benchmark test case in which the ground has no protruding features. Therefore, the ground surface roughness is modeled implicitly via wall functions for conducting CFD simulations on this test case. Proper application of boundary conditions at the inlet and ground surface is required to maintain horizontal homogeneity of the flow, i.e., for the flow at the inlet to be identical to that at the outlet.

Complexity 1, Homogeneous roughness: Array of blocks, similar to that used in BLWT, are used to model a highly simplified idealized built environment. The CFD results are compared against existing empirical formulas for estimating surface roughness parameters based on density and arrangement of obstacles.

Complexity 2, Inhomogeneous roughness: Multiple roughness patches with different characteristics are placed consecutively to model inhomogeneous roughness. The CFD results are compared against existing wind speed models for multiple roughness patches.

Complexity 3, Semi-idealized built environment: Simulations are conducted over a model that has typical features of a real built environment. The results are compared against wind tunnel test results of the same model in CEDVAL-LES (2011).

Complexity 4, Real built environment: Validation of simulation results on a real built environment is not in the scope of the present study, nonetheless, simulation is conducted on an area in

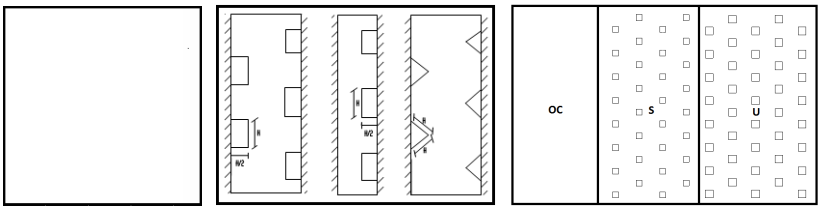

(a) Complexity-0 (b) Complexity-1 (c) Complexity-2

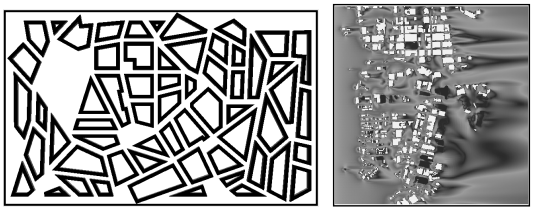

(d) Complexity-3 (e) Complexity-4

Fig. 1 Plan of different built environments showing the five categories of roughness considered in this study. The simplest case is an empty domain where the roughness is modeled implicitly, and the most complex is a real built environment where accurate prediction of the flow field is important

downtown Miami to briefly demonstrate the steps to be followed.

In the following, we describe the common choices made for conducting all the CFD simulations on the above mentioned built environment models. The software used for conducting simulations is an in-house finite-volume solver, which is now being extended to use high order discontinuous Galerkin (DG) method by the first author. The governing equations of fluid dynamics, i.e., the Navier-Stokes equations, can be solved only using a numerical procedure except in very simple flows where all the non-linear terms are dropped. For wind engineering applications, in which flows are of high Reynolds number, turbulence plays a major role. Therefore, a number of RANS turbulent models are implemented (Abdi and Bitsuamlak 2014b) including standard $k-\varepsilon$, RNG $k-\varepsilon$, Realizable $k-\varepsilon$ and $k-\Omega$. RANS models are often preferred in industrial applications because one is mainly interested in mean flow quantities. However, LES is becoming more and more feasible with the ever increasing computational power that has become available to the researcher and practicing engineers alike. The grid resolution required for resolving near-wall flows by LES maybe detrimental to speed of simulations, thus a hybrid RANS-LES approach can be used to resolve near-wall flow with unsteady RANS, and flow away from walls by LES. All the CFD simulations in this study are carried out with a steady state RANS model, namely the standard $k-\varepsilon$ model.

The code has also capability for generating block structured grids that will cover most of the case studies, Complexity 0 to Complexity 3. The last two cases, however, require a more complex grid generation software that takes a digital surface model in STereoLithography (STL) format as an input and produce a grid with higher refinement near the ground and building faces. The automatic hexahedral grid generation tool snappyHexMesh from OpenFOAM CFD (OpenFOAM 2013) is used for this purpose. Even though there is an abundance of tools for generating tetrahedral grids that are more suitable to finite-element calculations, an automatic hexahedral grid generator from irregular

surfaces is still an active research area. The process of grid generation using snappyHexMesh involves the following stages. First a background mesh is generated with refinement applied towards obstacles, and then part of the grid that lies outside of the computational domain is removed. After this stage, the ground surface is roughly established but it is still not yet smooth enough for final use. Therefore, a third stage of snapping to the surface is applied by moving vertices to surface planes. As a result, some of the cells near the surface may become deformed. For better accuracy and convergence, a final stage of adding prismatic layers of cells parallel to the surface is conducted in an iterative manner.

The computational domains are setup following recommendations for the use of CFD in wind engineering (Franke and Hirsch 2004). The length of the upstream region is fixed at 5H from the center of the first obstacle, where H is the height of the tallest obstacle. The outlet of the domain is placed 12H further downstream of the last obstacle so that outflow boundary condition can be assumed there for all flow quantities. The sides and top of the computational domain are placed 6H away from sides of the furthest obstacles to reduce blockage effects. These recommendations have been challenged since their first use, for instance, by Revuz *et al.* (2013) who argue that a domain of approximately 10% the volume of that suggested by the existing guidelines could be used with a loss in accuracy of less than 10%. Even though this latest recommendation have not been tried in the current study, the last test case considered, namely a simulation in downtown Miami area which has $>= 200$ m high buildings, can greatly benefit from it.

3. Complexity 0: Empty domain

CFD enjoys wide spread use in the wind engineering community; however, many parameters that influence simulation results are not well understood (Franke and Hirsch 2004). A rather trivial case that is commonly used to demonstrate the disparity between simulation results of different CFD software is the case of an empty domain. Due to the absence of obstacles, the characteristics of the wind should ideally be maintained along the whole length of the domain. However, the flow is rarely horizontally homogeneous unless proper boundary conditions are applied (Richards and Hoxey 1993, Hargreaves and Wright 2007, Blocken *et al.* 2007). This case serves as a benchmark for the rest of the case studies, and also to validate the in-house CFD code developed and used for this work.

3.1 Test setup

The computational domain used for this case study is the same as the one used by Hargreaves and Wright (2007). It has dimensions of 5000 m$\times$100 m$\times$500 m. The domain is meshed with 500$\times$50$\times$5 cells in which geometric expansions are applied in the vertical direction in such a way that the the size of nearest cell to the ground is 1 m. The criterion described in Blocken *et al.* (2007) that the height of the first cell's center (Z_p) be greater than the sand grain roughness ($K_s = 20z_0$) is satisfied for ground surface roughness length of z_0=0.01 m : Z_p=1 m $> K_s$=0.2 m. The reference wind speed is set at 10 m/s at a height of 6m. Various commonly used boundary conditions at the ground, inlet and top of the domain are considered to check if a horizontally homogeneous flow is obtained for CFD simulations done using the standard $k - \varepsilon$ turbulence model.

3.2 Boundary conditions

Boundary conditions are very important for any CFD simulation because they are cutoff planes that divide the area we are interested in studying from that we have no interest. In other words they are used to incorporate the influence of the surroundings in our model. The type of boundary condition also affects the placement of the cutoff planes relative to the central region of the domain where obstacles are placed. For example, use of symmetry boundary condition at the top and sides of the domain can introduce artificial accelerations unless the planes are placed far apart such that blockage ratio is kept below a specified minimum, about 3% (Franke and Hirsch 2004). The other issue concerns consistency of boundary conditions. The ground surface roughness, usually modeled implicitly via wall functions, should ideally lead to development of wind profiles that are exactly the same as those specified at the inlet (Richards and Hoxey 1993, O'Sullivan *et al.* 2011).

At the inlet of the computational domain fully developed equilibrium velocity and turbulence intensity profiles are applied based on upstream surface roughness characteristics (Miller and Davenport 1998, Wieringa 1993). The inlet wind profiles should be maintained in the upper portion of the computational domain until flow reaches the face of the object of study. This is very important for determination of wind load on buildings, which will otherwise be significantly different if, for instance, a uniform inlet velocity profile is used instead of logarithmic profile. A typical problem in ABL simulations is that maintaining horizontal homogeneity is not trivial to achieve with the current breed of CFD software. Richards and Hoxey (1993) have investigated the problem thoroughly and suggested boundary conditions (Eqs. (1)-(3)) to be specified at the inlet that will ensure horizontal homogeneity when the standard $k-\varepsilon$ turbulence model is used. Their formulas have been used by the wind engineering community for many years. The mean flow velocity u, turbulent kinetic energy k and turbulent dissipation ε are given as

$$u = \frac{u*}{\kappa} \ln \frac{z + z_0}{z_0} \tag{1}$$

$$k = \frac{{u*}^2}{\sqrt{C_\mu}} \tag{2}$$

$$\varepsilon = \frac{{u*}^3}{\kappa(z + z_0)} \tag{3}$$

where $u*$ is the frictional velocity, κ is the Von Karman constant, z_0 is the roughness length, z is the height above the ground and $C_\mu = 0.09$ is a constant in the $k-\varepsilon$ turbulence model.

Nikuradse's modified log-law equations are usually used as rough wall functions in many CFD code. In this case, the first cell should not lie within the equivalent sand grain roughness height, i.e., $Z_p > K_s$, as discussed in Blocken *et al.* (2007). This constraint is in conflict with using a fine mesh close to walls where high velocity gradients are present and turbulence is generated. One suggested remedy is to model the roughness explicitly, which is the approach used in the rest of the case studies in this work.

At the sides and top of the domain, a symmetry boundary condition that prevents both inflow and outflow is commonly used. The blockage ratio should be checked to avoid artificial accelerations in this case. Another remedy is to replace the boundary condition with one that allows for flow outwards through the boundary(Franke and Hirsch 2004). The common use of symmetry boundary condition

at the top of the boundary is rather unfortunate since it ignores the contribution of geostrophic wind in driving the ABL flow. Many researchers have noted that use of symmetry boundary condition results in stream-wise gradients of velocity profile. However, there are reasons why symmetry is assumed in many wind engineering problems. The major physical reason is that log layer in the ABL extends only up to a certain depth above which the gradient of velocity becomes zero. Also it is not known a priori what the values would be set at the top if symmetry boundary condition is not used. A shear stress boundary condition ($\tau = \rho u*^2$) should be applied at the top to get a homogeneous profile (Hargreaves and Wright 2007, Richards and Hoxey 1993). Another approach used by Blocken *et al.* (2007) is to apply Dirichlet boundary condition for velocity and turbulence quantities at the top.

3.3 Tests with different boundary conditions

Four different test cases, with different boundary conditions, are studied with regard to maintaining horizontal homogeneity of the flow. The ground surface roughness is said to be compatible with the inlet boundary condition if the flow at the inlet is maintained throughout the fetch.

Case 1 - Incompatible wall roughness
The first case applies the Richards and Hoxey (1993) boundary conditions at the inlet but assumes a smooth ground surface thereby creating a situation where the surface roughness exhibits a sudden change at the inlet. Due to this incompatibility, stream-wise gradients are observed in the profiles of U, k and ε as shown in Fig. 2. Close to the ground, both the velocity profile and turbulence dissipation show large changes as one goes downstream; while the profiles towards the top remain somewhat constant. On the other hand, the turbulent kinetic energy shows variations throughout. The difficulty of maintaining the turbulent kinetic energy along the fetch has been noted by Richards and Hoxey (1993) especially on the first cell close to the ground where many CFD software show peak values.

Case 2 - Compatible wall roughness
When surface roughness conditions compatible with the inlet profiles are applied, both velocity and turbulence kinetic energy profiles are maintained throughout the domain as shown in Fig. 3. The sand grain roughness used for the simulation is determined according to the relation K_s=20z_0=0.2 m. However the calculated turbulent kinetic energy profile still shows variations from the expected constant vertical profile.

Case 3 - Fixed U,k and ε at the top
From the previous simulations, we observe that the flow quantities at the top show some variations due to the imposed symmetry boundary condition. Blocken *et al.* (2007) has suggested using Dirichlet boundary condition to make sure that the flow quantities remain the same at least at the top of the boundary. The result for this case is shown in Fig. 4. While velocity and turbulence dissipation show an almost perfect fit from start to finish of the fetch, the turbulent kinetic energy profile show some variations from the expected uniform profile.

Case 4 - Uniform k and ε at the inlet
It is customary to specify constant values of k and ε at the inlet for convenience. The assumption is

Table 1 Summary of empirical formulas for estimating roughness length z_0. The frontal area density ratio λ_f is the ratio of the frontal area to the planar area of obstacles. H is the height of the blocks, and C_d is the drag coefficient

Model	$\frac{z_0}{H}$
Lettau (1969)	$0.5\lambda_f$
Counihan (1971)	$1.08\lambda_f - 0.08$
Theurer (1993)	$1.6\lambda_f(1 - 1.67\lambda_p)$
MacDonald *et al.* (1998)	$(1 - \frac{d}{H})\exp(-(0.5\frac{C_d}{k^2}((1 - \frac{d}{H})\lambda_f)^{-0.5})$

correct for k but not for ε. The simulation result for this case shows a developing ε profile along the fetch, before reaching more or less the same values at the outlet, as shown in Fig. 5. So far we have managed to get homogeneous horizontal velocity (U) and turbulent dissipation (ε) profiles. To get a homogeneous turbulent kinetic energy (k) profile, further modifications to wall functions are necessary. Most commercial CFD code do not usually offer wall functions that can maintain horizontally homogeneous k profile, however we note that it is possible to achieve this behavior through further modifications of wall functions that involve changes in the finite volume discretization as described in Hargreaves and Wright (2007). From the cases we have considered so far, the third case that fixes the flow quantities at the top of the domain and uses the Richards and Hoxey conditions gives the best results.

4. Complexity 1: Homogeneous array of blocks

The next higher level of complexity in our idealized built environment study is that of homogeneous roughness due to regular array of obstacles. Simulations shall be carried out on regular and staggered array of blocks for wind coming from different angles. The arrangements of the roughness blocks are chosen to be symmetric, so that a significant reduction of the computational domain to a much smaller section of one or two rows is possible, as shown in Fig. 6. The results from these simulations will be compared against existing empirical models for estimation of roughness length z_0, summarized in Table 1.

4.1 Test setup

The test setup used for this study is similar to that used by MacDonald *et al.* (1998). Regular and staggered arrays of cubes are exposed to wind coming from different directions, and velocity profiles are recorded at different locations behind the obstacles. Wind speed profiles typically show variations in the transverse direction, because some of the locations are sheltered by the blocks while the others lie in the gap between the blocks. Therefore, average of velocity profiles at multiple locations in the transverse direction is used to get a representative velocity profile for a given section (such as A-A shown in Fig. 7). This approximation gives acceptable results for regular arrays of cubes, but it may be inaccurate for staggered and other irregular arrangements. Close to the ground and right behind an obstacle, the velocity profile can reverse due to flow recirculation, while at locations close to center line of gap the flow continues forward. The averaging operation on a cross section removes these variations in direction of velocity and hence positive velocity profiles are observed also at heights

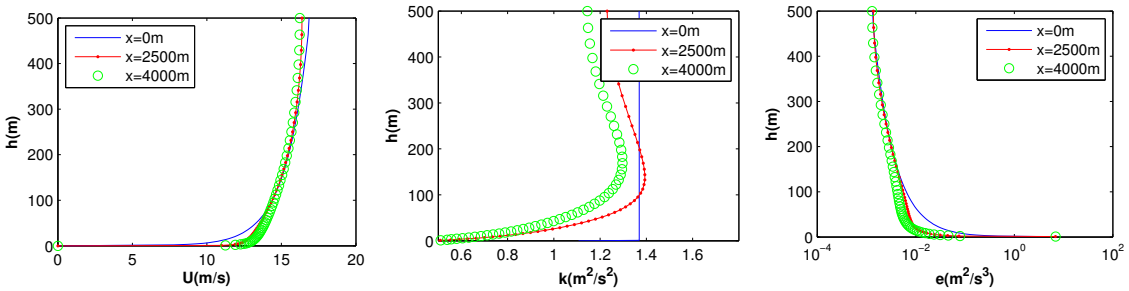

Fig. 2 Profiles of horizontal velocity, turbulent kinetic energy and dissipation for case 1

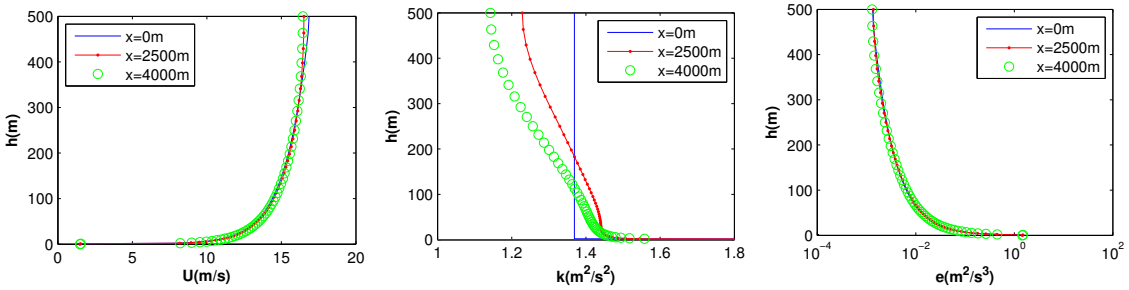

Fig. 3 Profiles of horizontal velocity, turbulent kinetic energy and dissipation for case 2

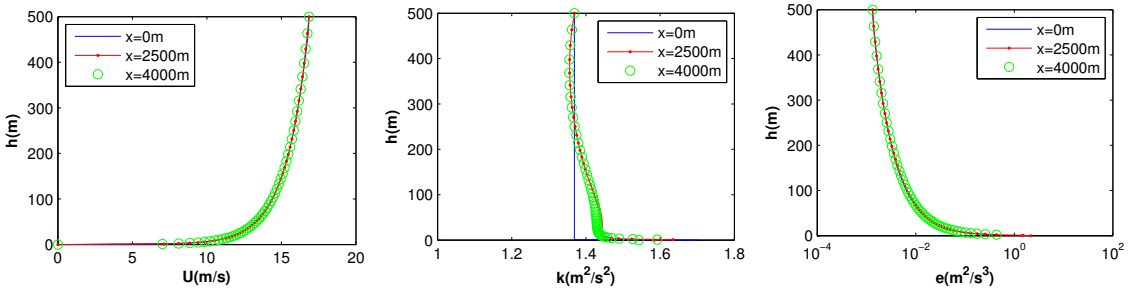

Fig. 4 Profiles of horizontal velocity, turbulent kinetic energy and dissipation for case 3

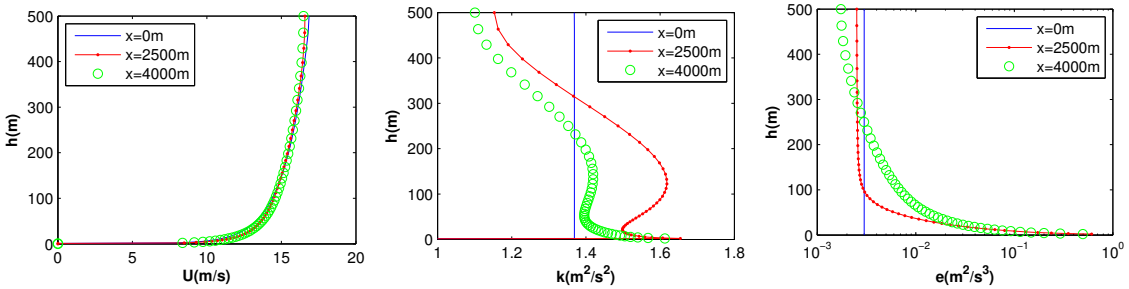

Fig. 5 Profiles of horizontal velocity, turbulent kinetic energy and dissipation for case 4

where recirculation happens.

Simulations are conducted for various configurations of obstacles with different spacing, regular and staggered arrangement, and different wind angle of attacks as shown in Fig. 6. Symmetry of arrangement of obstacles is exploited to reduce the computational domain. Only one row of obstacles are needed for uniformly arranged obstacles and two rows for the staggered obstacles case. Then models are prepared for six area density ratios (0.05, 0.11, 0.16, 0.2, 0.33, and 0.5) for all configurations of obstacles considered so that variation of roughness parameters (z_0 and d) with area density ratio can be plotted. The area density ratio for the different cases are calculated using the following formula

$$\lambda = \frac{1}{(1 + \frac{S}{H})^2} \tag{4}$$

For example, a spacing S=1.5H between blocks gives $\lambda = 0.16$. Accordingly the roughness length is estimated as $z_0 = 0.5\lambda H = 0.08H$ by Lettau's model, and about $0.093H$ using Counihan's model etc. Absolute values of roughness length can be obtained by substituting the height of block used for this study $H = 20$ m.

4.2 Results and discussion

Our goal is to calculate the roughness parameters, namely roughness length and displacement height, from velocity and turbulence intensity profiles obtained from CFD simulations. As mentioned before, the average of wind profiles at five locations, shown in Fig. 7, is considered instead of a single wind profile measurement. The roughness parameters are determined using equations from Lo (1990) listed in Eqs. (7)-(6). The value of d obtained using this method is usually satisfactory, however the value of z_0 can be very sensitive to the selected reference height in the inner layer. Given a non-dimensionalized reference height z_n and corresponding wind speed u_n, first we determine the displacement height d iteratively using Eq. (6), and then subste d in Eq. (7) to get the roughness length

$$\alpha = \frac{1}{1 - u_n}, \beta = \frac{u_n}{1 - u_n}, \text{ and } A = \int_0^1 U(z)dz. \tag{5}$$

$$(1 - A - d)\ln(1 - d) - (1 - d) + (A - 1 + d)[\alpha \ln(z_n - d) - \beta \ln(1 - d) + \frac{(z_n - d)^\alpha}{(1 - d)^\beta}] = 0 \tag{6}$$

$$z_0 = \frac{(z_n - d)^\alpha}{(1 - d)^\beta} \tag{7}$$

The results from the CFD simulations are briefly summarized as follows. The first observation is that the boundary layer grows with fetch length until it becomes fully developed at some downstream location. This is usually achieved within the first few rows of blocks, about 7 rows, which is significantly smaller than the total number of rows that is 30. The roughness parameters obtained indirectly from velocity profiles of CFD simulations are shown in Fig. 8. Estimates of roughness parameters

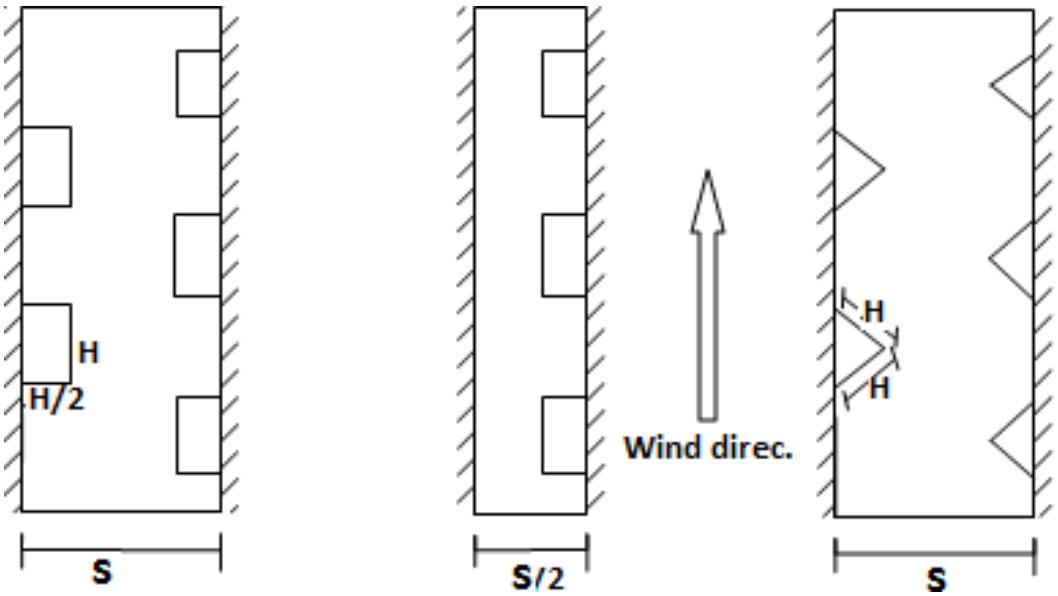

Fig. 6 Plan of different homogeneous roughness configurations showing symmetry planes (hatched). staggered array of blocks that requires two rows of half blocks(left), regular array of blocks with one row of half blocks (middle), and triangular array of blocks (right)

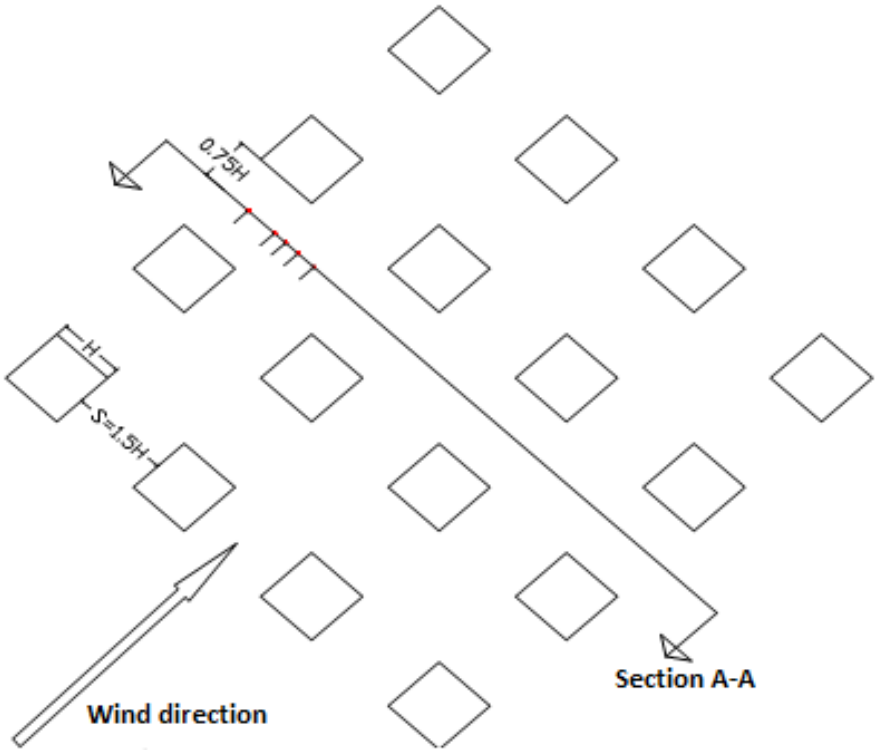

Fig. 7 Plan of regular array of cubes with height H and spacing 1.5H also showing location of probes behind obstacles

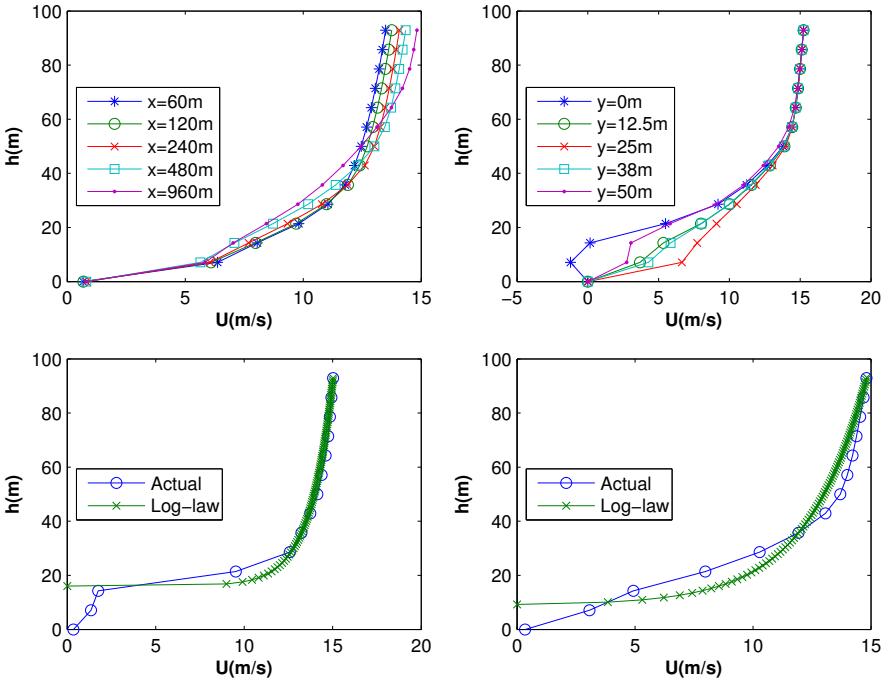

Fig. 8 Spatial variation of velocity profiles along the longitudinal x-direction (topleft), along the transverse y-direction (top right). The bottom figures show an examples of logarithmically fitted velocity profiles ('Log-law') using the observed data ('Actual') by using Lo's formula in Eq. (6) . **h** is the height above the ground

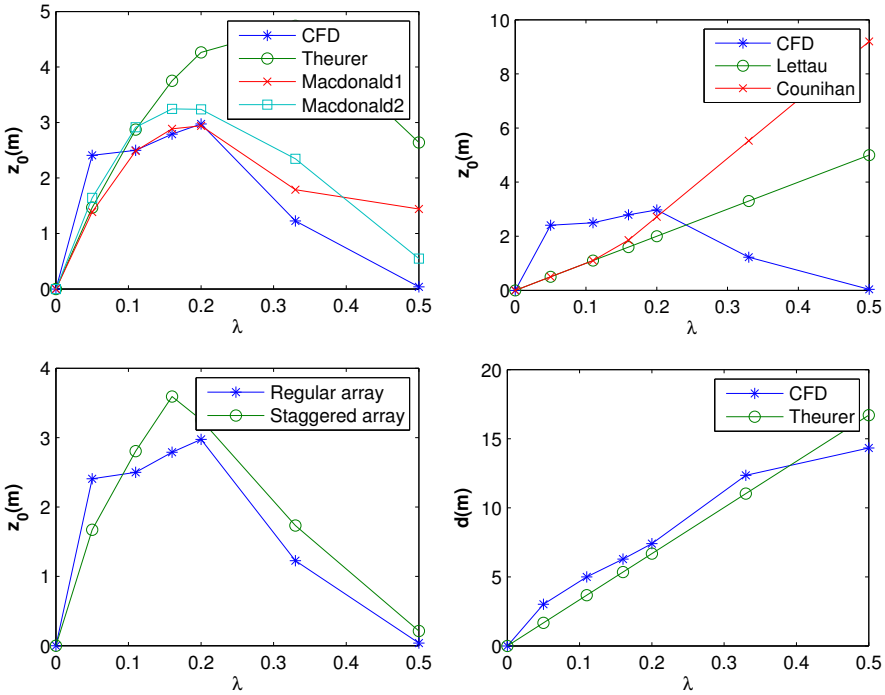

Fig. 9 Comparison of roughness parameters, roughness length (top) and displacement height (bottom-right), obtained from CFD simulations against existing empirical models. Bottom right figure compares result of CFD with regular and staggered array of cubes. The x-axis represents area density ratio λ

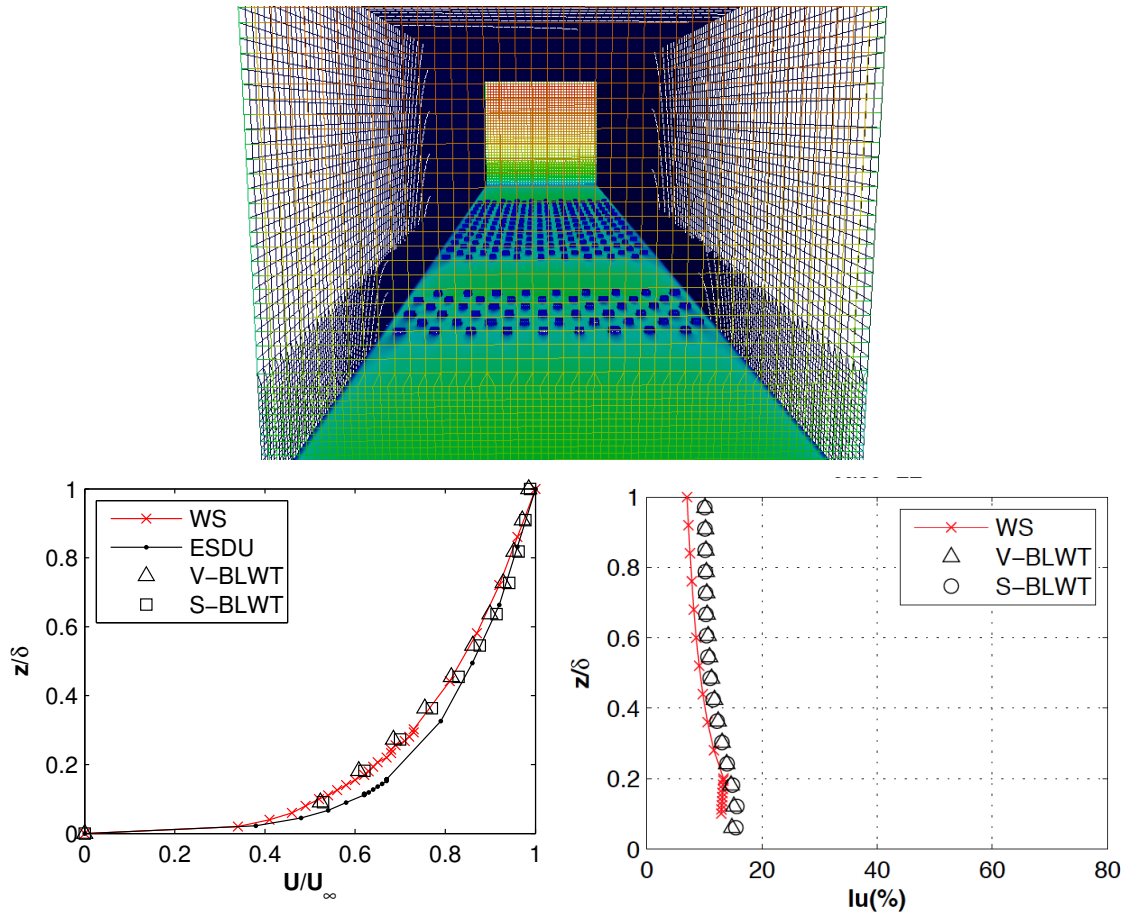

Fig. 10 Virtual wind tunnel(top) for inhomogeneous roughness simulation, and comparison of velocity profile (bottom left) and turbulence intensity profile (bottom right) results obtained from CFD simulation vs those obtained from empirical models, namely, Wang and Stathopoulos (WS) and ESDU models (right)

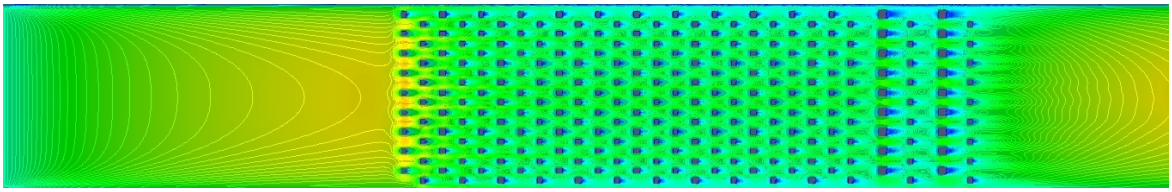

Fig. 11 Plan of inhomogeneous roughness configuration with 5 patches in a virtual wind tunnel. The patches are placed going upwards starting from a downstream location close to the turntable: 1 row (125 m) suburban, 1 row (125 m) urban, 1 row (125 m) suburban, 1 row (125 m) urban, and 24 rows (2 km) urban

obtained from different empirical models, listed in Table 1, are also shown in the same figure for comparison. The most promising model, namely McDonald roughness model, is tested in two ways in which the displacement height is calculated differently. The first method determines roughness length from displacement height calculated using Lo's equation, henceforth called $McDonald1$. The second method uses d calculated from Theurer's equation, henceforth called $McDonald2$. The $McDonald1$ method seems to give the best fit to the CFD calculated result as shown in Fig. 9, followed by $McDonald2$ model confirming superiority of this model. The Theurer model also shows good fit up to area density ratio of 20% but deteriorates afterwards. Lettau's and Counihan's models significantly underestimate the roughness length for area density below 20% and overestimate it for area density larger than 20%.

The staggered array of obstacles and the case of regular arrays 45° wind angle of attack both resulted in higher roughness compared to the simple case of regular arrays as shown in Fig. 9. The staggered placement of obstacles increase roughness due to relatively larger exposure of faces of the cubes to the oncoming wind. A regular array of cubic obstacles exposed to a 45° oncoming wind can be considered to be equivalent to a staggered array of triangular obstacles as shown in Fig. 6. We can also observe that the deviation of Lettau's and Counihan's models from CFD model is less pronounced on staggered array of blocks compared to that on regular arrangement. This is probably due to less wake interference in the case of staggered arrangement that needs larger spacing between blocks for a given roughness length, thus the flow becomes isolated for each roughness block. However Lettau's and Counihan's model still show significant deviations from the CFD model, which is partly explained by the larger drag imposed by the cubic obstacles (C_D=1.2).

5. Complexity 2: Inhomogeneous array of blocks

Surface roughness is rarely homogeneous over a long fetch, instead it can exhibit significant variations within short distances. For example, in downtown Miami, the characteristic of wind coming from the ocean experiences a sudden change in roughness from open (ocean) to urban (coastal community) and then to suburban within a few miles. These local, small scale roughness changes have significant effect on the velocity and turbulence intensity profiles. Wang and Stathopoulos (2007) have conducted extensive BLWT tests over multiple roughness changes from which was derived a wind speed model, henceforth called WS-model, that improved upon the existing ESDU-82026 (1993) model. In this section, we conduct CFD simulation on an inhomogeneous array of blocks, i.e., by placing multiple homogeneous roughness patches consecutively. Wind speed profiles are measured at the end of the last roughness patch, and then the CFD results are compared with the above mentioned empirical wind speed models.

5.1 Test setup

The model considered here, shown in Fig. 11, has five roughness patches of different characteristics (length, packing density): (2 km, suburban), (125 m, urban), (125 m, suburban), (125 m, urban) (125 m, suburban). The packing density for each roughness class, which is homogeneous, is determined a priori by conducting multiple simulations with a chosen block arrangement until the desired velocity and turbulence intensity profiles are obtained. The empirical formulas from Table 1 are used to get an initial guess for the density of packing of blocks. The first CFD simulations

models the whole BLWT, henceforth called a Virtual Boundary Layer Wind Tunnel (V-BLWT). The V-BLWT used for this case is the one used by Wang and Stathopoulos (2007) for their experimental investigation of inhomogeneous roughness, namely Concordia University BLWT that has a working section of 12.2 m x 1.8 m x 1.8 m. Roughness blocks were used to model suburban and urban roughness, while carpet was used to represent open country roughness. For the CFD simulations, open country roughness of z_0 =0.024 m is modeled implicitly via wall functions, and suburban and urban roughness are modeled explicitly via roughness blocks. The height of blocks for suburban and urban roughness are set to 5.08 cm and 7.62 cm respectively, with a center-to-center spacing of 0.3 m for both. A reduction in computational demand can be achieved by taking advantage of the symmetry of arrangement of blocks, a Symmetric Virtual Boundary Layer Wind Tunnel (S-BLWT). An extensive test on various inhomogeneous roughness configurations can be found from the authors previous work (Abdi and Bitsuamlak 2014a).

5.2 Boundary conditions

At the inlet a logarithmic velocity profile with $U_{ref} = 12.5$ m/s at a height of $H_{ref} = 0.6$ m is applied. A homogeneous roughness of $z_0 = 0.024$ m is used for the open-country roughness, and blocks of 5.08 cm and 7.62 cm high are used to model suburban and urban roughness respectively. The length scale of the BLWT simulation is 1:400 and the time scale is 3:400. At the sides and top of the computational domain, smooth wall boundary condition are used. The profiles of k and ε at the inlet are determined according to Richards and Hoxey (1993) formulas. At the outlet an outflow boundary condition is used. For the S-BLWT simulation, with one row of blocks, symmetry boundary condition is assumed at the sides of the domain.

5.3 Results and discussion

The results obtained from the CFD simulation, Fig. 10, show good agreement with the Wang and Stathopoulos Model (WS) model than the ESDU model. This is interesting because the WS model is verified with wind tunnel tests, and the ESDU model is derived from 2D CFD simulations. A two dimensional CFD study conducted by Wang and Stathopoulos (2007), using empirical formula to model the shear stress variation due to roughness change, concluded that CFD shows better agreement with ESDU model than the WS model. The current work using explicit roughness modeling approach matches the experimentally derived WS better than it does the numerically derived ESDU model. As mentioned before, symmetry can be exploited to reduce the model to effectively a single row of roughness elements (S-BLWT). The results obtained for this case are almost identical to the V-BLWT results for both wind speed and turbulence intensity profiles. Thus, a significant reduction in computational resources is achieved, without degrading accuracy of simulations. The S-BLWT method can not be used when the test object breaks symmetry of the model or when more complex turbulence models, such as LES, are used.

6. Complexity 3: Semi-idealized urban environment

So far the cases considered focused on determining average roughness characteristics of highly idealized built environment models. This is acceptable in situations where detailed wind flow characteristics inside the built environment are not of high importance. For example, in BLWT

testing, the building of interest and its surrounding within a short radius are modeled as accurately as possible, whilst the rest of the model is replaced with regular array of blocks that have similar average roughness characteristics. Studies concerning pollutant dispersion and pedestrian level wind comfort in built environment require a more detailed model of the built environment. Therefore, next we consider a semi-idealized urban canopy model (Fig. 12), which is heterogeneous and morphologically consistent with a typical central European city characteristics (Hertwig *et al.* 2012). It has sharp building corners, open courtyards, plazas and complex intersections. CFD simulations are conducted over this model and comparison of wind speed profiles inside the domain are made between CFD and wind tunnel measurements. Detailed BLWT test results are available from CEDVAL-LES (2011), which is a compilation of wind-tunnel datasets intended for validation of LES based numerical flow and dispersion models. This study uses RANS turbulence models; therefore, only the time-averaged statistics from the database are used for comparison instead of the whole time series data.

6.1 Test setup

The online database has two cases of Complexity 3, one case in which all roofs are flat and another where some of the roofs are slanted. The flat roofs case is chosen for this study. The computational domain is setup similar to Hertwig *et al.* (2012), who conducted numerical simulations using various CFD software and compare the results with the wind tunnel dataset. The model tested in the boundary layer wind tunnel has a scale of 1:225, with the full scale size representing an area of 1320 m$\times$820 m$\times$24 m. The computational domain is of size 1672 m$\times$1140 m$\times$144 m. A background mesh of 191$\times$118$\times$41 is applied first, and then transferred to snappyHexMesh for refinement towards the surface of buildings and the ground. This automatic grid generation tool takes the urban surface model in STereoLithography (STL) format as an input and then forms layers of hexahedral elements towards the surface through an iterative process. The total number of cells after all refinements are applied is about 4 million.

6.2 Boundary conditions

At the inlet a logarithmic velocity profile with $U_{ref} = 6.537$ m/s at a height of $H_{ref} = 144$ m is applied. A homogeneous roughness of $z_0 = 0.06$ m is used for the ground, and hence the friction velocity is $U_* = 0.346$ m/s. At the sides of the computational domain a symmetry boundary condition is used, and at the top the values of U, k and ε are fixed to the same value used for the inlet at the same height: $U = 6.537$ m/s, $k = 1.057$ m^2/s^2, $\varepsilon = 0.0049$ m^2/s^3. The profiles of k and ε are determined according to Richards and Hoxey (1993) formulas. At the outlet an outflow boundary condition is used.

6.3 Results and discussion

Plots of velocity contours at different heights within the urban canopy of height 24 m is shown in Fig. 13. The wind field is sampled at 40 locations distributed uniformly across the area in an 5 rows$\times$8 columns. Densely spaced measurements are also taken within the core of the model to characterize street canyon flow, but we compare only normalized vertical velocity profiles at the 40 locations. A comparison between boundary layer wind tunnel and CFD simulation results are shown in Fig. 14. We can observe that there is in general good agreement between the two methodologies, but there are

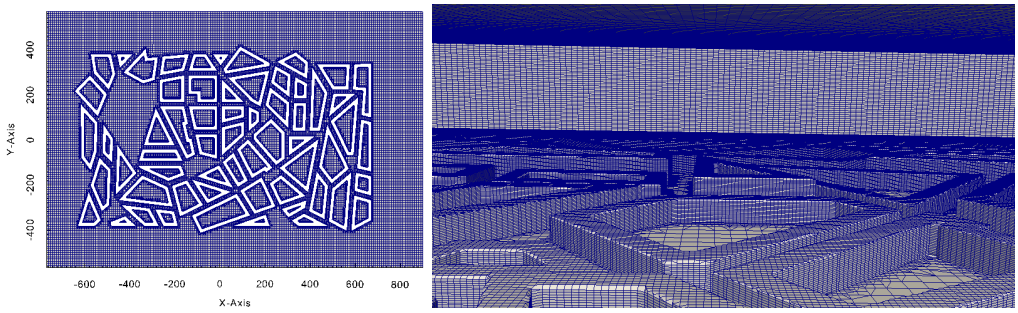

Fig. 12 Plan of semi-idealized urban model (left) and close-up view of section of the grid (right)

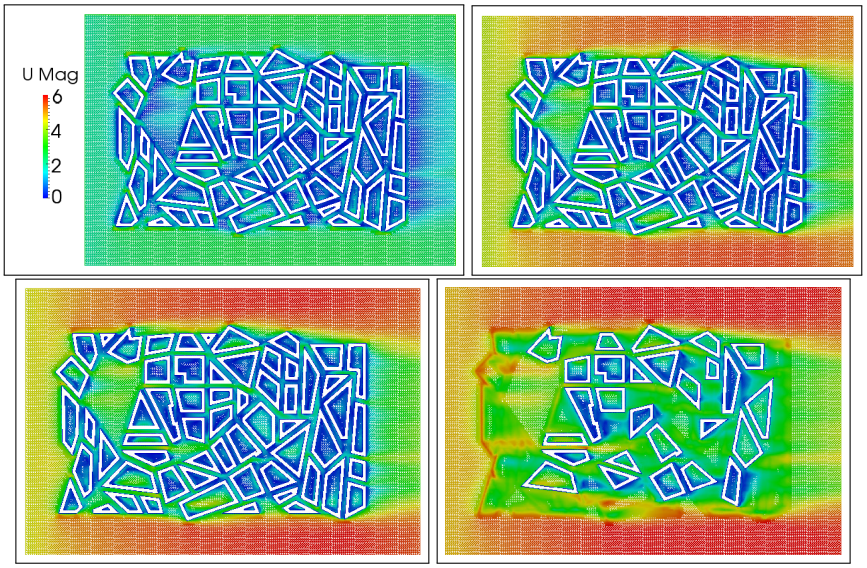

Fig. 13 Velocity color contours at 2 m, 9 m, 12 m and 18 m heights. The color contours indicate that velocity increases (becomes more red) with height

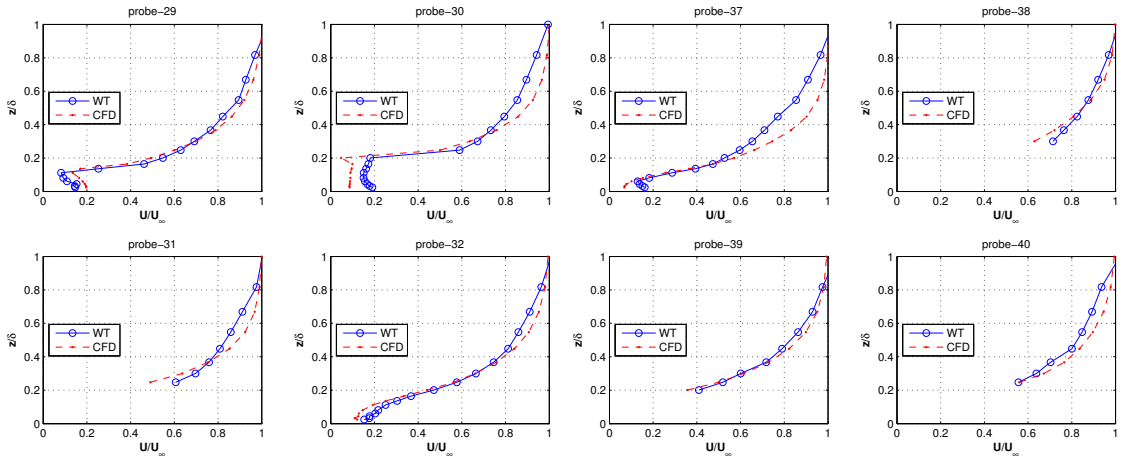

Fig. 14 Comparison between CFD and BLWT for some probe locations inside the model. The x-axis is normalized velocity and y-axis is normalized height

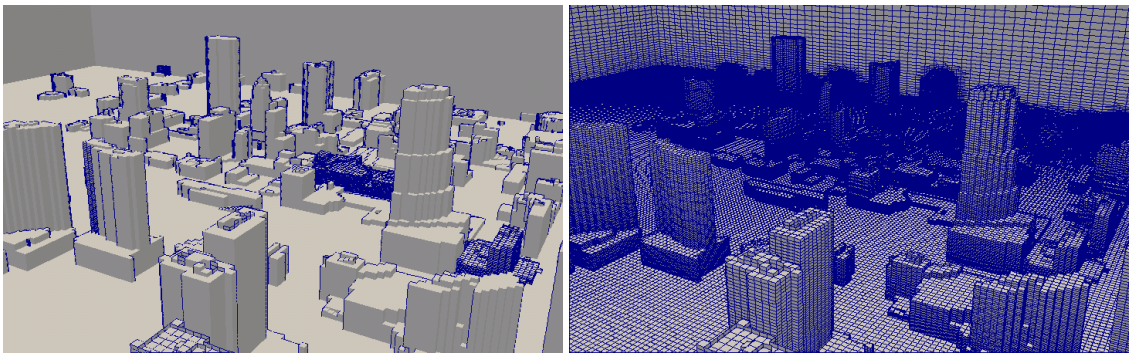

Fig. 15 Building edges of the STL file (left) and corresponding surface mesh generated using snappyHexMesh (right)

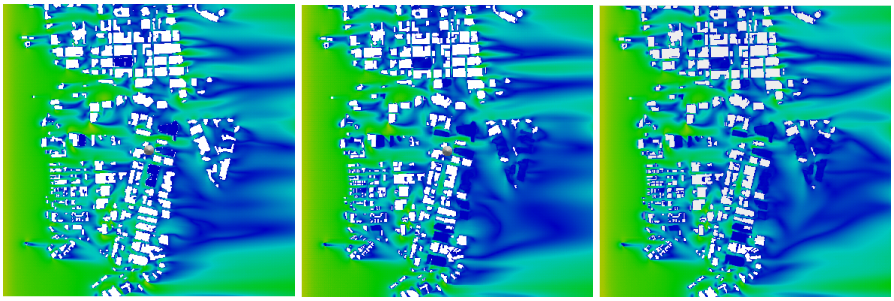

Fig. 16 Partial grid independence check using velocity contours at 5 m height by varying number of cells in the vertical direction 30 cells(left), 60 cells (middle) and 90 cells(right)

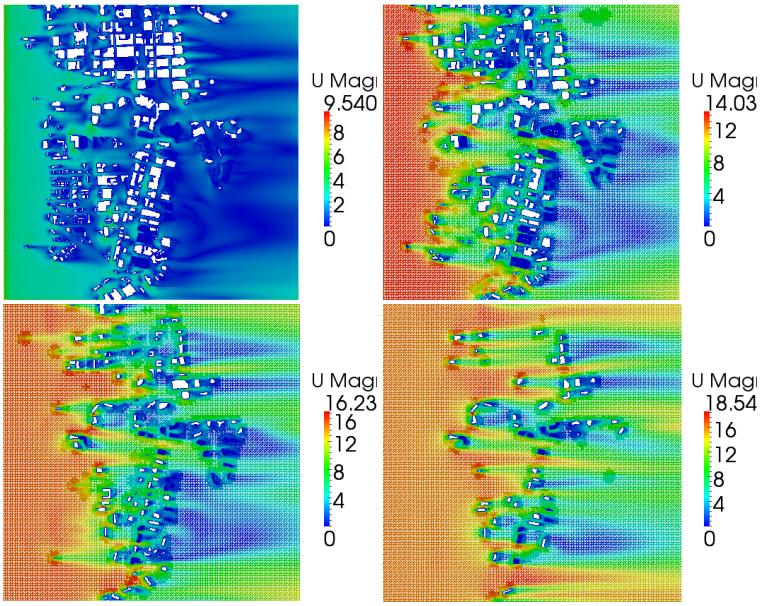

Fig. 17 Velocity contours at different heights: z=0 m (top left), z=50 m (top right),z=100 m (bottom left), z=200 m (bottom right)

also few cases, e.g., probes 37 and 30, that indicate significant differences can be obtained in canopy regions.

7. Complexity 4: Real built environment

The next higher level of complexity is a real built environment that is classified as Complexity 5 by CEDVAL-LES dataset. Data for validation is not available for this case, hence its purpose is merely for demonstrating the procedures to be followed for real built environment studies. The selected built environment is an area in downtown Miami which has some high rise buildings of height $\geq$ 200 m. The computational domain has dimensions of 4.3 km$\times$4.3 km$\times$2 km. Micro-scale simulations of this magnitude need to consider the effect of Coriolis force since some buildings penetrate well into the Ekman layer; however, this is ignored for the current simulations. The boundary layer height is chosen to be 2 km to reduce blockage effect due to the high rise buildings in the area.

7.1 Test setup

First a background mesh of 120$\times$120$\times$60 cells is generated, which is then passed to snappyHexMesh for refinement close to the ground and building faces. The final grid, after all refinements are applied, consisted of 2.3 million cells. The grid generation process involves three stages : clipping, snapping to surface, and layer additions for better boundary layer simulations. The final prismatic layer addition stage was problematic for this particular case, producing cells of high skewness and similar low quality cells, so the result after the second stage, i.e., snapping to surface, is retained for the current simulation. Snapshot of the background STL surface edges of building and the corresponding mesh is shown in Fig. 15.

7.2 Boundary conditions

At the inlet a logarithmic velocity profile for a rough surface condition is assumed mainly because field observation data was not available and the upstream terrain resembles a mildly rough environment from visual inspection. If field observation data were available for the inlet profile, the correct procedure would be to make logarithmic fitting of inlet velocity profile followed by modification of the standard $k - \varepsilon$ model constants as discussed Blocken *et al.* (2011a), Martinez (2011). Symmetry boundary conditions are assumed at the sides and top of the computational domain. The ground surface is assumed to be no-slip with roughness of $z_0 = 0.1$.

7.3 Results and discussion

Velocity contour plots at pedestrian level and higher are shown in Fig. 16. The simulations are re-run with different grid sizes in the vertical direction to check for partial grid independence of results. The number of cells in the vertical direction is changed from 60 to 30 and 90 cells for a total of 1.2 million cells and 3.2 million cells respectively. The result with 30 cells in the vertical direction shows some qualitative differences with the current 60 cells case; however, the larger 90 cells case did not show significant differences. Therefore, it can be said that partial grid independence has been achieved with the current grid size of 60 cells in the vertical direction. Even though grid independence studies can be time consuming, they should be carried out for all built environment studies using CFD.

The velocity contour at different elevations, shown in Fig. 17, suggest that wind speed increases with height and that the flow pattern changes significantly. The planar area density ratio of obstacles decreases with height because only few of the buildings reach heights of $\geq$ 200 m. This leads to a reduction of drag force with height which leads to higher wind speeds. Micro-scale simulations of built environments of this size, that do not cover the whole area, pose a problem with regard to application of boundary conditions. For example, many buildings at the sides of the computational domain have been cut; hence, the assumption of symmetry boundary condition at the sides is not appropriate.

8. Conclusions

This work has investigated effect of roughness on wind flow in built environment models of various level of complexity using CFD simulations. The study started from the simplest case, namely, an empty domain with ground surface roughness modeled implicitly via wall functions. This case is intended solely for benchmarking and selecting appropriate boundary conditions. Then, arrays of roughness blocks arranged in regular and staggered manner are placed on the ground to model roughness explicitly. The results from the CFD simulations are compared against existing empirical formulas for estimating roughness parameters based on arrangement and density of packing of blocks. The CFD results showed the best agreement with the MacDonald *et al.* (1998) empirical model, specially at higher packing densities in which other empirical models failed to give good predictions. The next case considers the effect of multiple roughness changes within short distances. Three uniform roughness patches, from the previous case, are placed consecutively and CFD simulations are carried out to determine wind profiles at the end of the last patch. The results from CFD simulation are compared against two wind speed models, namely, the WS and the ESDU model. CFD showed better agreement with the WS which was also verified using wind tunnel tests unlike the ESDU model that is developed solely from 2D CFD simulations.

So far the focus has been on determining average roughness characteristics to be used in cases where detailed wind flow characteristics inside the built environment are not important. In built environment studies such as pollutant dispersion and pedestrian level wind comfort studies, a more detailed model of the built environment is required. Thus, the next higher level model considered for this purpose is a semi-idealized built environment model, taken from CEDVAL-LES (2011) data base, that has the morphological characteristics of a typical European city. Simulations are carried out using this model and the results, wind speed profiles at designated locations inside the domain, are compared with wind tunnel test results. The results show fairly good agreement confirming feasibility of CFD methodology for conducting detailed wind flow simulations in complex built environment. Finally, the case of a real built environment is considered using a model in an area in downtown Miami. Validation data was not available for this case, which is often the case for most other complex built environment studies as well, thus only qualitative comparisons are made.

In conclusion, this study has investigated various idealized models of the built environment, where CFD results are compared in an averaged sense (roughness) for the first three cases, and detailed wind profile comparisons inside the domain for the semi-idealized built environment case. The CFD simulations results are found to be in good agreement with the corresponding validation method for each of the cases. For complexity-0 case, empty domain, comparison of CFD simulation

conducted with the standard $k-\varepsilon$ model has shown excellent agreement with theory as long as proper boundary conditions are used. For complexity 1 case, homogeneous roughness, CFD results have shown good agreement with some of the empirical models tested in this study at different packing densities. For complexity 2 case, inhomogeneous roughness, 3D CFD simulations conducted in a virtual wind tunnel have shown good agreement with wind tunnel derived models, even though past research done with 2D simulations have indicated differences as high as 20% can be observed. For complexity 3 case, semi-idealized built environment, the wind speed profiles obtained at multiple probe locations have shown good agreement even though significant differences are observed in some of the locations in the canopy region. The last case, real built environement, could not be verified due to lack of validation data; therefore, the conclusions made here concern only the idealized and semi-idealized test cases.

References

Abdi, D. and Bitsuamlak, G. (2014a), "Numerical evaluation of the effect of multiple roughness changes", *Wind Struct*., **19**(6), 585-601.

Abdi, D. and Bitsuamlak, G. (2014b), "Wind flow simulations on idealized and real complex terrain using various turbulence models", *Adv. Eng. Softw*., **75**, 30-41.

Aboshosha, H., Bitsuamlak, G. and Damatty, A.E. (2015), "LES of ABL flow in the built-environment using roughness modeled by fractal surfaces", *Sustainable Cities Soc.*, **19**, 46-60.

Asghari, M. (2014), "Experimental and analytical methodologies for predicting peak loads on building envelopes and roofing systems", PhD thesis, Florida International University.

Blocken, B. and Carmeliet, J. (2002), "Spatial and temporal distribution of driving rain on a low-rise building", *Wind Struct.*, **5**(5), 441-462.

Blocken, B. and Carmeliet, J. (2004a), "Pedestrian wind environment around buildings: Literature review and practical examples", *J. Therm. Envcir. Build. Phys.*, **28**(2), 107-159.

Blocken, B. and Carmeliet, J. (2004b), "A review of wind-driven rain research in building science", *J. Wind Eng. Ind. Aero.*, **92**(13), 1079 -1130.

Blocken, B., Janssen, W. and Hooff, T. (2011), "CFD simulation for pedestrian wind comfort and wind safety in urban areas: General decision framework and case study for the Eindhoven university campus", *Environ. Model. Softw.*, **28**, 15-34.

Blocken, B., Stathopoulos, T. and Carmeliet, J. (2007), "CFD simulation of the atmospheric boundary layer: wall function problems", *Atmospher. Envir.* **41**(2), 238-252.

Blocken, B., Stathopoulos, T., Carmeliet, J. and Hensen, J. (2011), "Application of CFD in building performance simulation for the outdoor environment: an overview", *J. Build. Perform. Simulation* **4**(2), 157-184.

CEDVAL-LES (2011), "Compilation of experimental data for validation of micro-scale dispersion models", *Meteorological Institute*, University of Hamburg, Germany.
URL: *http://www.mi.zmaw.de/index.php?id=6339*

Counihan, J. (1971), "Wind tunnel determination of the roughness length as a function of the fetch and roughness density of three dimensional roughness elements", *Atmospher. Envir.* **5**(8), 637-642.

Davenport, A., Grimmond, C., Oke, T. and Wieringa, J. (2000), "Estimating the roughness of cites and sheltered country", *Proceedings of the 12th American Meteorological Society Conference On Applied Climatology*.

ESDU-82026 (1993), *Strong winds in the atmospheric boundary layer, Part 1: hourly-mean wind speeds*, Engineering Science Data Unit.

Franke, J. and Hirsch, C. (2004), "Recommendations on the use of CFD in wind engineering", *Proceedings of the International Conference in Urban Wind Engineering and Building Aerodynamics*.

Hall, D., Macdonald, R., Walker, S. and Spanton, A. (1996), "Measurements of dispersion within simulated urban arrays: A small scale wind tunnel study", *BRE Client Report CR 178/96*.

Hansen, F. (1993), "Surface roughness lengths", ARL Technical Report U.S. Army, *White Sands Missile Range, NM* 88002-5501.

Hargreaves, D. and Wright, N. (2007), "On the use of k-epsilon model in commercial CFD software to model the atmospheric boundary layer", *J. Wind Eng. Ind. Aerod.*, **95**, 355-369.

Hertwig, D., Efthimiou, G., Bartzis, J. and Leitl, B. (2012), "CFD-RANS model validation of turbulent flow in a semi-idealized urban canopy", *J. Wind Eng. Ind. Aerod.*, **111**, 61-72.

Huang, H., Ooka, R., Chen, H., Kato, S., Takahashi, T. and Watanabe, T. (2008), "CFD analysis on traffic-induced air pollutant dispersion under non-isothermal condition in a complex urban area in winter", *J. Wind Eng. Ind. Aerod.*, **96**(10), 1774-1788.

Lettau, H. (1969), "Note on aerodynamic roughness parameter estimation on the basis of roughness element description", *J. Appl. Meteorol.*, **8**(5), 828-833.

Lo, A. (1990), "On the determination of zero-plane displacement height and roughness length for flow over forest canopies", *Bound. Layer Meteorol.*, **51**(3), 225-268.

MacDonald, R., Griffiths, R. and Hall, D. (1998), "An improved method for the estimation of surface roughness of obstacle arrays", *Atmos. Environ.*, **32**(11), 1857-1864.

Martinez, B. (2011), "Wind resource in complex terrain with openfoam", Master's thesis, Technical University of Denmark.

Miller, C. and Davenport, A. (1998), "Guidelines for the calculation of wind speed ups in complex terrain", *J. Wind Eng. Ind. Aerod.*, **74-76**, 189-197.

OpenFOAM (2013), "Openfoam, the open source CFD toolbox". **URL:** *http://www.openfoam.com/*

O'Sullivan, J., Archer, R. and Flay, R. (2011), "Consistent boundary conditions for flows within the atmospheric boundary layer", *J. Wind Eng. Ind. Aerod.*, **99**(9), 66-67.

Revuz, J., Hargreaves, D. and Owen, J. (2013), "On the domain size for the steady-state cfd modelling of a tall building", *Wind Struct.*, **15**(4), 313-329.

Richards, P. and Hoxey, R. (1993), "Appropriate boundary conditions for computational wind engineering models using the k-epsilon turbulence model", *J. Wind Eng. Ind. Aerod.*, **46**, 145-153.

Tang, W. and Davidson, C. (2004), "Erosion of limestone surfaces caused by wind-driven rain: Numerical modeling", *Atmos. Environ.*, **38**(33), 5601-5609.

Theurer, W. (1993), "Dispersion of ground level emissions in complex built-up areas", PhD thesis, University of Karlsruhe.

Tominaga, Y. and Stathopoulos, T. (2011), "CFD modeling of pollution dispersion in a street canyon: Comparison between les and rans", *J. Wind Eng. Ind. Aerod.*, **99**(4), 340-348.

Wang, K. and Stathopoulos, T. (2007), "Exposure model for wind loading of buildings", *J. Wind Eng. Ind. Aerod.*, **95**(9-11), 1511-1525.

Wieringa, J. (1993), "Representative roughness parameters for homogeneous terrain", *Bound. Lay. Meteorol.*, **63**(4), 323-363.

Wright, N. and Hargreaves, D. (2013), *Environmental applications of Computational Fluid Dynamics*, second edn, John Wiley and Sons.

CC